A Three-Phase Controlled-Current PWM Converter with Leading Power Factor

BOON TECK OOI, SENIOR MEMBER, IEEE, JOHN C. SALMON, JUAN W. DIXON, AND ASHOK B. KULKARNI

Abstract—**Experimental tests performed on a three-phase bipolar-transistor controlled-current PWM power modulator show that it can operate with near-sinusoidal currents at 60 Hz with a 360-degree power angle range. Because of its capability to operate with leading power factor and good waveform, the PWM converter is a promising alternative to the thyristor Graetz bridge. A theoretical method based on the concept of "local average" is presented.**

INTRODUCTION

THE PUNITIVE tariffs levied by utilities against excessive vars and the threat of stricter harmonic standards have recently aroused interest in the forced-commutated converters [1]–[6]. Up to now the line-commutated thyristor converter has remained unchallenged in the world of variable-speed drive systems. However, it is becoming clear that the costs and the ample cabinet space requirements of the capacitors and the filters, which have to be installed for power factor and harmonic improvements, should be considered together with the cheapness of the line-commutated thyristor circuits. With the falling prices of fast-switching high-power transistors, MOSFETS, and GTO's, one sees in the offing the possibilities of PWM converters replacing the classical line-commutated thyristor converter.

This paper describes the capabilities and the operational limitations of an experimental controlled-current bipolar-transistor three-phase PWM power modulator when operated as a converter. The laboratory model is constrained by a limited university research budget to low power ratings. However, the results reported here have universal applications by resorting to the usual scaling laws.

The performance characteristics are promising because not only are the current waveforms substantially sinusoidal, but the modulator is also capable of working with a 360-degree range of power angle. The practical implications are exciting. Up to now researchers have been pressing towards only a unity power factor operation. The experimental findings show that it is possible to work with a leading power factor and thus the converter can be applied to improve the overall power factor of the plant. The ability of forced-commutated circuits to circulate leading or lagging vars without the presence of physical capacitor or inductor banks is known and has found applications in the utility environment [7].

Part I describes the tests and the experimental characteristics of the PWM modulator. Part II presents theoretical correlations of certain test results using a new analytical approach based on the idea of the "local average." Because the ability to operate at leading power factor is a distinctive merit, both experimental and analytical effort has been directed towards establishing that this capability does not come from the filter capacitor across the dc link. This is felt to be necessary because the theorem concerning circulating vars in [7] is so general that one needs to show that this specific controlled-current PWM modulator qualifies to be within its scope.

Paper IPCSD 86-20, approved by the Static Power Converter Committee of the IEEE Industry Applications Society for presentation at the 1985 Industry Applications Society Annual Meeting, Toronto, ON, Canada, October 6–11. This work was supported in part by the Natural Science and Engineering Research Council of Canada and in part by the Ministry of Education, Province of Quebec, through an FCAC grant. Manuscript released for publication June 25, 1986.

B. T. Ooi, J. W. Dixon, and A. B. Kulkarni are with the Department of Electrical Engineering, McGill University, 3480 University Street, Montreal, PQ, Canada H3A 2A7.

J. C. Salmon is at 22 Bartle Road, St. Andrew's Square, London, W11 1RF England.

IEEE Log Number 8611182.

PART I—PERFORMANCE CHARACTERISTICS

The Experimental Facility

The PWM modulator was adapted from a controlled-current PWM inverter that had been built in the laboratory for experiments with variable-speed ac motors. As the operation of the controlled-current mode has been described in [8]–[11] it is necessary to refer here only to the three important changes that had been made to: 1) the ac system, 2) the dc link, and 3) the generation of the waveform templates.

AC System

A three-phase balanced voltage source at supply frequency replaced the ac motor load. As shown in Fig. 1, three-phase variable tap autotransformers provided control of the magnitude of the voltage $\tilde{V}$ from the 60-Hz mains.

The external impedances of $\tilde{Z} = R + j\omega L\ \Omega$ had been added to the lines. Some line inductances are needed because their Ldi/dt voltages form an essential element in forcing the currents through the back-biased free-wheeling diodes during "regeneration." It is the capability of the PWM modulator to work in the "regenerative mode" that enables it to function as a converter.

This paper uses the convention of the inverter so that the ac current $\tilde{I}$ is assumed to flow out of the modulator. Thus the phase voltage $\tilde{V}_m$ at the modulator terminal of Fig. 1 is given by the equation

$$\tilde{V}_m = \tilde{V} + \tilde{Z}\tilde{I}. \tag{1}$$

The large values of $\tilde{Z} = 0.42 + j3.93\ \Omega$ had been used in

0093-9994/87/0100-0078$01.00

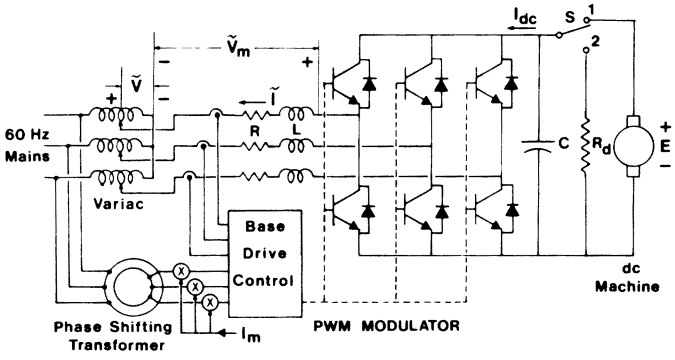

Fig. 1. Schematic of experimental three-phase controlled-current PWM converter.

the experiments to ascertain that the influence of their voltage drops was measurable. Conceivably, in the practical system, $\tilde{Z}$ would include the impedances of the line and the leakage reactances of transformers.

DC Link

In order that the dc link was capable of bilateral power conversion in the program of tests, the dc link voltage was taken from the armature terminals of a separately excited dc machine driven by an induction motor. In all the measurements the field current was adjusted so that the dc link voltage was regulated to $E = 60$ Vdc. For proper operation E must be sufficiently high so as to back-bias the free-wheeling diodes. As shown in Fig. 1 the current direction for I_{dc} follows that of the inverter convention. A capacitor C provided filtering at the dc link.

Current Waveform Templates

The controlled-current feature of the modulator consists of monitoring the output current of each phase and using the ON–OFF switchings of the bipolar transistors to ensure that the measured current tracks the template waveform i_R within a narrowly defined window width I_w. Fig. 2(a) shows a modulator current being maintained within the bounds $i_R \pm 0.5I_w$, the template current being substantially constant for the time scale chosen.

Fig. 1 shows that the template waveforms were taken from the ac mains. The control of the phase angle was introduced through a three-phase phase-shifting transformer. The outputs of the phase-shifting transformers were multiplied by the signal I_m so that the template waveform was $i_R = I_m \sin(\omega t + \phi)$.

Part I—Experimental Tests

The tests had been planned to evaluate the PWM modulator as a component in a variable-speed drive system. Its primary function is to rectify three-phase ac power from the mains to a dc link. The dc link may be connected to a variable-frequency inverter ac motor drive or to a chopper dc motor drive. During regenerative braking of the motors the dc link current reverses in direction and the converter should be able to return power to the utility. The static tests showed that the laboratory model measured up to these duties.

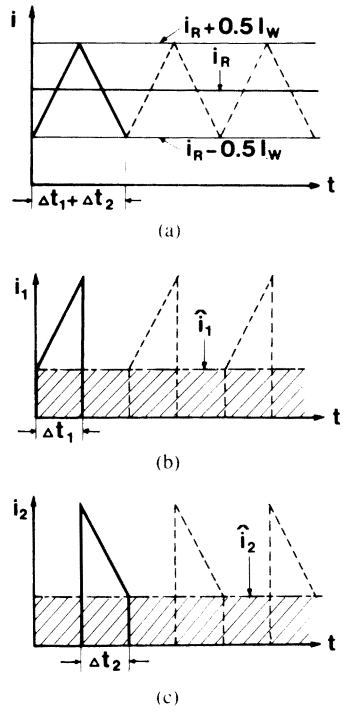

Fig. 2. (a) Modulator output being switched between bounds to track template signal. (b) Instantaneous current, and local average at upper dc link. (c) Instantaneous current, and local average at lower dc link.

360-Degree Power Angle Range

Fixing the template waveform magnitude I_m at a constant value, the phase-shifter was used to adjust the phase angle over the range 0–360°. The modulator delivered near-sinusoidal currents over the full 360° power angle range. The photographs in Fig. 3 are records of the ac phase voltages and currents. Figs. 3(a) and 3(b), respectively, show the modulator operating at unity power factor as an inverter ($\phi = 0°$) and as a converter ($\phi = 180°$). In Fig. 3(c) the modulator was functioning as a switchmode capacitor ($\phi = 270°$).

From the photographs, one observes that the ac harmonics were in the high frequency range, which are relatively cheap to filter. The current in the dc link was a constant value for each phase angle. Power transistor switching ripples overrode it, but as they are at high frequencies the filter capacitor requirement is modest.

Converter/Inverter Reversibility at Fixed Power Angle

As part of a variable-speed drive the power reversals are expected to occur at a fixed power angle. A test was performed in which the phase angle was fixed at 0° and the magnitude control I_m was varied from positive to negative values passing through zero. As observed through the oscilloscope the amplitude of the current waveform of Fig. 3(a) diminished until it became a "flat" zero as shown in Fig. 4. Then it underwent a 180° phase reversal and the amplitude increased with the waveform shown in Fig. 3(b).

Self-Support Voltage Capability at DC Link

The tests reported so far had been conducted with the voltage across the dc link being provided by the dc machine

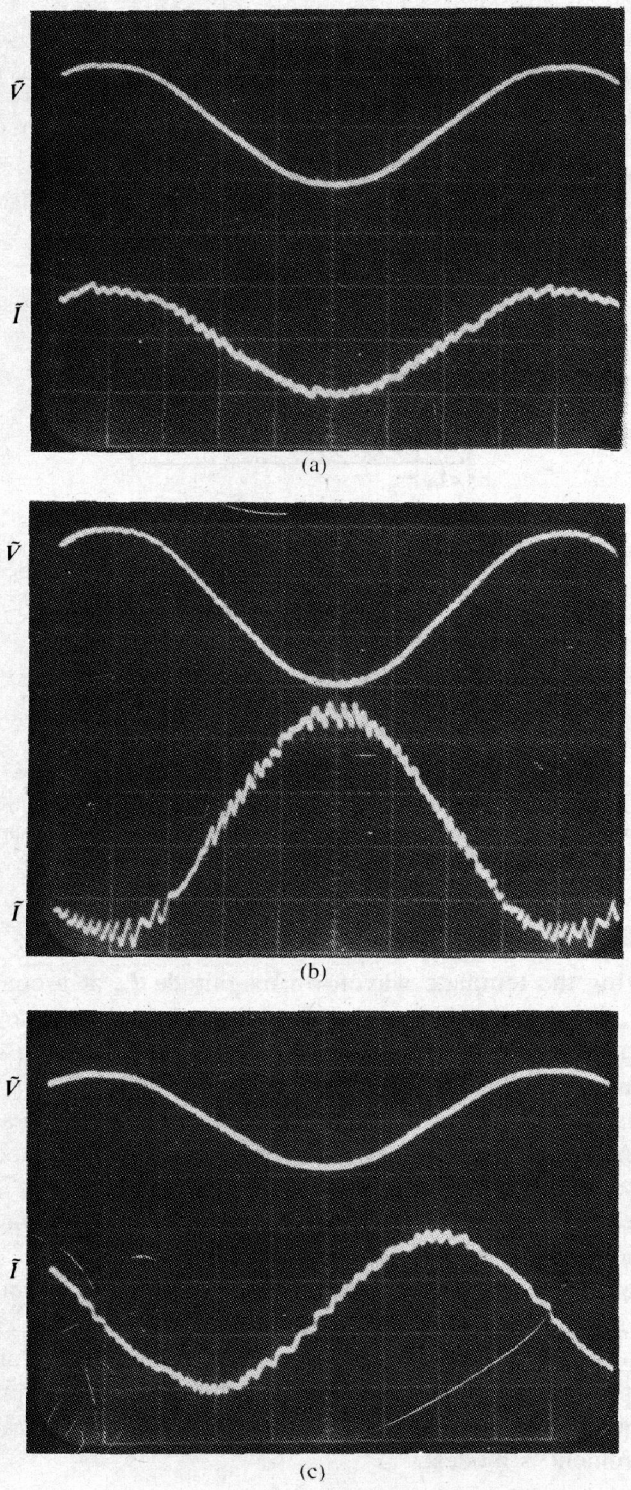

Fig. 3. Phase voltage and current. (a) $\emptyset = 0°$, inversion at unity power factor. (b) $\emptyset = 180°$, conversion at unity power factor. (c) $\emptyset = 270°$, operation as switchmode capacitor.

(induction motor driven). In the operational system the dc link voltage should be provided by the charges across the filter capacitor and maintained at a desired voltage level by the converter.

To prove this capability, once the modulator was operating satisfactorily as a converter the dc machine was disconnected by switching S in Fig. 1 from position 1 to position 2. In position 2 the switch S connected a resistance R_d across the filter capacitor C. For the purpose of the test the resistance R_d served as a crude representation of the inverter or chopper load.

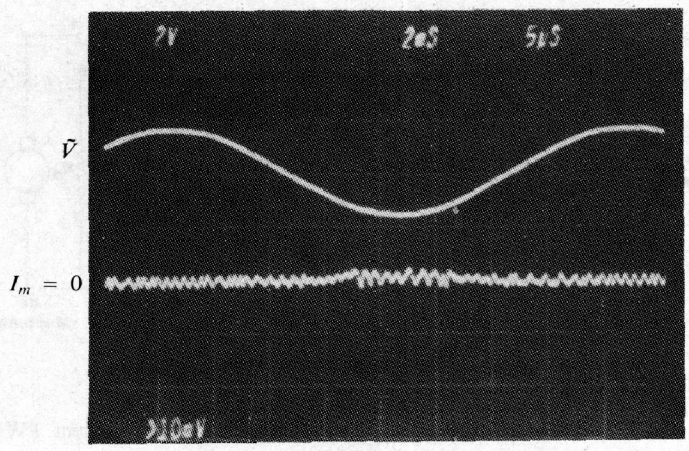

Fig. 4. Modulator current at zero amplitude.

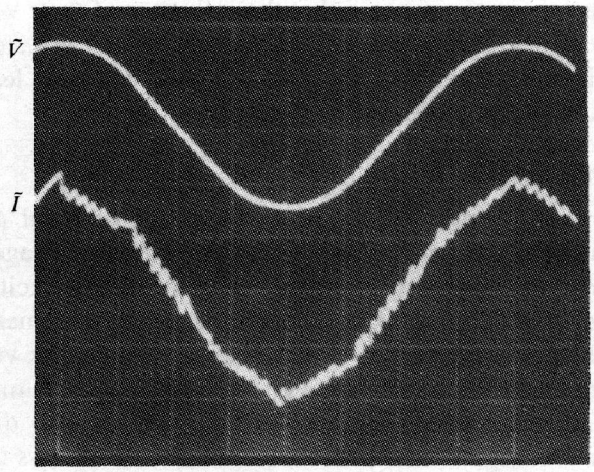

Fig. 5. Modulator current showing waveform distortion.

It was found that the dc link voltage was self-supporting through the charge across the filter capacitor and the modulator continued to function without mishap. The dc voltage increased by increasing the settings of I_m.

Current Waveform Distortion Limit

For the circuit configuration of Fig. 1 the theoretical estimate of the current waveform distortion limit has been computed as:

$$|\tilde{V}_m| = \frac{E}{\sqrt{6}} . \tag{2}$$

When the ac phase voltage at the modulator $\tilde{V}_m$ has a magnitude that exceeds the limit defined in (2) there is insufficient resultant voltage to force the currents through the inductances so as to track the sinusoidal template waveforms. Fig. 5 shows an instance of this current distortion.

The experiment was designed with two purposes in mind: 1) to give experimental verification to the theoretical limit of equation (2) and 2) to investigate how the limit can be applied to the ac network design.

The experimental procedure was as follows. The switch S was set back in position 1 so that the dc link voltage was provided by the dc machine, which was regulated at $E = 60$ V. The magnitudes of the ac phase currents were set by the template control to 2 A. For each power angle ϕ the auto-

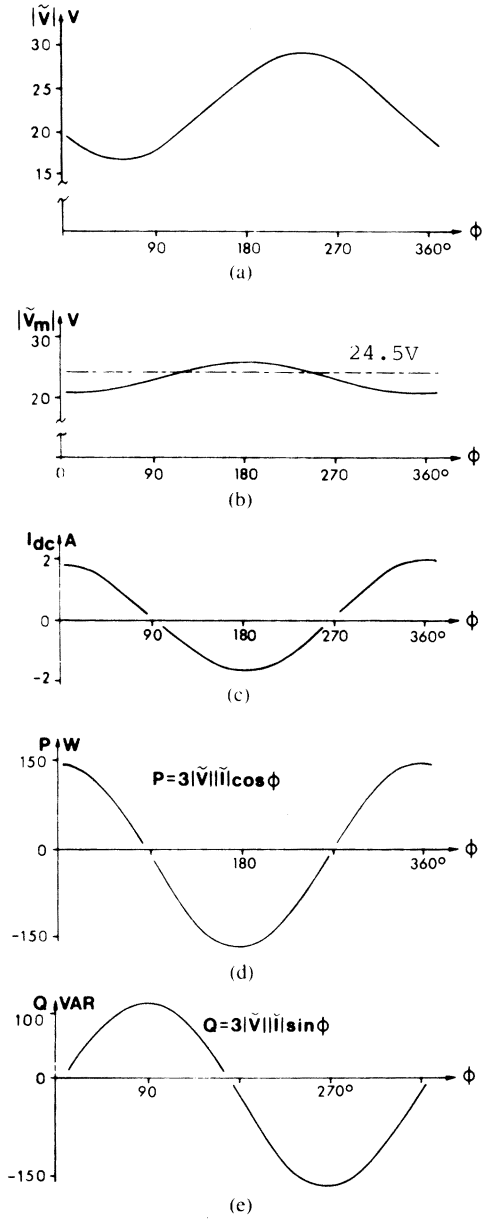

Fig. 6. Experimental measurements as function of phase angle ∅. (a) Magnitude of ac phase voltage at autotransformer. (b) Magnitude of ac phase voltage at modulator terminal. (c) DC link current. (d) Real power from ac source. (e) VAR's from ac source.

transformer voltage $\tilde{V}$ was adjusted until the current distortion started to become noticeable to the eye. The measurements from the experiment are shown in Fig. 6.

Fig. 6(a) shows $|\tilde{V}_m|$ plotted as a function of ϕ. The curve of $|\tilde{V}_m|$ versus ϕ in Fig. 6(b) is obtained by application of (1). Since E = 60 V, based on (2), the current waveform distortion limit should be 24.5 V. There is a slight discrepancy, and the reason for it is evident when one compares the deviations of $|\tilde{V}_m|$ from 24.5 V in Fig. 6(b) with the measurements of the dc current which are plotted in Fig. 6(c). It is apparent that (2) must be corrected for a dc voltage drop associated with the dc current passing through a resistive element. The resistance is that of the transistors (for positive I_{dc}) and that of the diodes (for negative I_{dc}). More accurate instrumentation and more detailed and complete characterizations of equivalent resistances of transistors and diodes are needed for better agreement. For practical purposes it is possible to conclude that the experimental data give justification to (2).

The implication of the current waveform distortion limit is that the dc link voltage should be operated at as high a voltage as the breakdown limits of the components permit.

The second conclusion is that the critical ac voltage is $\tilde{V}_m$, right at the ac terminals of the modulator, and this can be computed from any balanced ac voltage source (such as $\tilde{V}$) using conventional ac circuit theory (such as in (1)).

Loss of Control Limit

When the ac source voltages were increased in magnitude slightly beyond the current waveform distortion limit of (2) the PWM modulator lost its controlled-current capability altogether. This limit did not exist in inverter experiments when the ac terminals of the modulator were connected to an induction motor because the motor consists of passive elements. However, when the motor was replaced by ac voltage sources, $\tilde{V}$ as shown in Fig. 1, the six "free-wheeling" diodes could form a rectifier bridge when the diodes went into conduction.

The current controllability of the PWM modulator depends on the voltage of the dc link being sufficiently high so as to back bias the free-wheeling diodes.

No attempt was made to measure the limit accurately. An estimate of the limit is based on the formula of the output dc voltage of the six-pulse diode rectifier bridge:

$$V_{dc} = \sqrt{6}\,|\tilde{V}_m|\,\frac{3}{\pi}. \tag{3}$$

Loss of control limit is expected when

$$V_{dc} > E \tag{4a}$$

$$|\tilde{V}_m| > \frac{E}{\sqrt{6}}\,\frac{\pi}{3}. \tag{4b}$$

VAR Availability

The ability to operate the converter at a leading power factor is a very attractive feature. It is necessary to show conclusively that this capability does not come from the capacitor of the dc link.

From the data of Fig. 6(a) and with $|\tilde{I}|$ = 2 A, the real power $3|\tilde{V}||\tilde{I}|\cos\phi$ and the reactive power $3|\tilde{V}||\tilde{I}|\sin\phi$ were computed and plotted in Figs. 6(d) and 6(e), respectively. Since E = 60 V_{dc}, the dc current curve of Fig. 6(c) is also the curve of the dc power.

At ϕ = 90° and 270°, small positive dc currents in Fig. 6(c) showed that the resistive losses in the ac circuit and across the transistor and diodes were supplied by the power from the dc machine. However, at the two neighboring points where I_{dc} = 0, one sees in Fig. 6(e) that large positive and negative reactive voltamps circulated in the PWM modulator without entering the dc link to the capacitor.

A comparison of Figs. 6(c) and 6(d) shows that the power balance equation

$$EI_{dc} = 3[|\tilde{V}||\tilde{I}| \cos \phi + |\tilde{I}|^2 R]$$

is approximatly satisfied, with no allowance for the reactive power in the dc link.

The possibility of the reactive power appearing as current ripples in the dc link is discounted by the theory discussed in Part II.

Part II—Analysis: Method of Local Average

The method of "local average" is presented here to prove two properties that have been experimentally observed in the three-phase controlled-current PWM modulator.

Property 1: The dc link current is time-invariant (except for switching ripples).

Property 2: The var's do not enter the dc link.

The theoretical development proceeds in three steps: 1) single-phase modulator, 2) three single-phase modulators, and 3) open neutral configuration. It is assumed that the transistors and diodes are ideal switch elements and, likewise, $\tilde{v}$, E, and L are ideal circuit elements.

Step 1: Single-Phase Modulator

The single-phase PWM modulator is modelled as shown in Fig. 7. Fig. 2 shows, on an expanded time frame, the current waveform of i as it tracks the template waveform i_R within the window width I_w. In the time segment Δt_1, the current i flows through transistor T1, rising from $i_R - 0.5I_w$ to $i_R + 0.5I$. Then the transistor is switched off and in time segment Δt_2 the current in the inductance L is continued through the free-wheeling diode D2. It is assumed that $\Delta t_1 + \Delta t_2$ is so brief that i_R is substantially constant.

In the successive switchings the currents i_1 and i_2 of the center-tapped power supplies $E/2$ are trains of roughly trapezoidal pulses shown in Figs. 2(b) and 2(c).

It is proposed here that each pulse train be characterized by a local average, the time span of the average being $\Delta t_1 + \Delta t_2$. Thus the local average of $\hat{i}_1$ is defined as

$$\hat{i}_1 = \frac{\int_0^{\Delta t_1} i \, dt}{\Delta t_1 + \Delta t_2} \approx \frac{i_R \Delta t_1}{\Delta t_1 + \Delta t_2} \tag{5}$$

while the instantaneous value of i_1 is

$$i_1 = i \quad \text{in the time span } \Delta t_1$$

$$i_1 = 0 \quad \text{in the time span } \Delta t_2.$$

The local average $\hat{i}_1$ is the value given by (5) in the time span $\Delta t_1 + \Delta t_2$.

Likewise, one defines a local average for $\hat{i}_2$ and it is evaluated as

$$\hat{i}_2 = \frac{i_R \Delta t_2}{\Delta t_1 + \Delta t_2}. \tag{6}$$

The "local averages" are illustrated in Figs. 2(b) and 2(c).

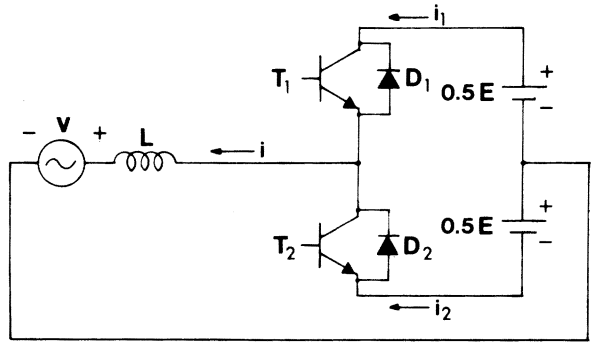

Fig. 7. Single-phase PWM modulator.

Switching Times: When the transistor T1 conducts:

$$L di_1/dt = 0.5E - v. \tag{7}$$

The transit time Δt_1 for the current to cross from $i_R - 0.5I_w$ to $i_R + 0.5I_w$, based on (7), is:

$$\Delta t_1 = \frac{L \Delta I_w}{0.5E - v}. \tag{8}$$

When the diode D2 conducts:

$$L di_2/dt = -(0.5E + V) \tag{9}$$

and based on (9)

$$\Delta t_2 = \frac{L \Delta I_w}{0.5E + v}. \tag{10}$$

Local Average Formulae: Substituting (8) and (10) into (5) and (6)

$$\hat{i}_1 = \frac{(0.5E + v)}{E} i_R \tag{11}$$

$$\hat{i}_2 = \frac{(0.5E - v)}{E} i_R. \tag{12}$$

It should be mentioned that although (11) and (12) have been derived for positive values of i_R, their formulae remain unchanged for negative values of i_R. For negative values of i_R, i_1 flows through D1 and i_2 through T2.

Ideal Controlled-Current PWM Modulator Assumption: When the switching rates are very fast, one can make $I_w \to 0$, $\Delta t_1 + \Delta t_2 \to 0$, and $i \to i_R$. In this ideal situation, one can treat the local averages $\hat{i}_1$ and $\hat{i}_2$ as continuous time functions.

DC Link Currents: Substituting

$$v = \sqrt{2}\, V \sin \omega t \tag{13}$$

$$i = \sqrt{2}\, I \sin (\omega t + \phi) \tag{14}$$

into (11) and (12),

$$\hat{i}_1 = 0.707 I \sin (\omega t + \phi) + \frac{VI}{E}[\cos \phi - \cos (2\omega t + \phi)] \tag{15}$$

$$\hat{i}_2 = 0.707I \sin(\omega t+\phi) - \frac{VI}{E}[\cos\phi - \cos(2\omega t-\phi)]. \quad (16)$$

The dc link current therefore has a fundamental line frequency and a second harmonic component riding on a dc component.

DC Power: The power delivered by the dc sources is

$$P = 0.5E(\hat{i}_1 - \hat{i}_2) = VI[\cos\phi - \cos(2\omega t+\phi)]. \quad (17)$$

AC Power: The power consumed by the ac source is

$$P = (\sqrt{2}V \sin\omega t)(\sqrt{2}I \sin(\omega t+\phi)) = VI[\cos\phi - \cos(2\omega t+\phi)]. \quad (18)$$

From (17) and (18) one sees that the concept of "local average" current yields the same formula for ac and dc power.

Step 2: Single-Phase Modulator

Minimal changes are required of the theoretical development when one considers the single-phase modulator of Fig. 7 connected as shown in Fig. 8. To each of the variables v, i, i_1, and i_2 designated in Fig. 7, the subscripts A, B, and C are added to indicate that they belong to each of the balanced three phases. Thus the balanced ac voltages and currents are:

$$\begin{aligned} v_a &= \sqrt{2}V \sin\omega t \\ v_b &= \sqrt{2}V \sin(\omega t-120°) \\ v_c &= \sqrt{2}V \sin(\omega t-240°) \quad (19) \\ i_A &= \sqrt{2}I \sin(\omega t+\phi) \\ i_B &= \sqrt{2}I \sin(\omega t+\phi-120°) \\ i_C &= \sqrt{2}I \sin(\omega t+\phi-240°). \quad (20) \end{aligned}$$

Substituting (19) and (20) into (15) one has

$$\begin{aligned} \hat{i}_{1A} &= 0.707I \sin(\omega t+\phi) + \frac{VI}{E}[\cos\phi - \cos(2\omega t+\phi)] \\ \hat{i}_{1B} &= 0.707I \sin(\omega t+\phi-120°) + \frac{VI}{E}[\cos\phi - \cos(2\omega t+\phi-240°)] \\ \hat{i}_{1C} &= 0.707I \sin(\omega t+\phi-240°) + \frac{VI}{E}[\cos\phi - \cos(2\omega t+\phi-480°)]. \quad (21) \end{aligned}$$

Since

$$\sin\theta + \sin(\theta-120°) + \sin(\theta-240°) = 0 \quad (22)$$

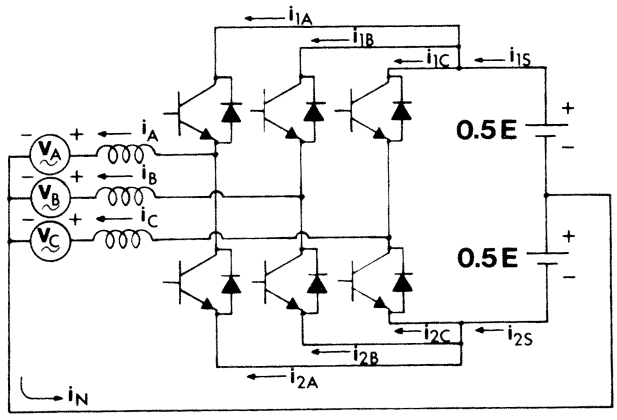

Fig. 8. Synthesis of three-phase version of Fig. 7.

and

$$\cos\theta + \cos(\theta-240°) + \cos(\theta-480°) = 0 \quad (23)$$

it follows the sum of the upper three branches of the dc link yields:

$$\hat{i}_{1S} = \hat{i}_{1A} + \hat{i}_{1B} + \hat{i}_{1C} = 3\frac{VI}{E}\cos\phi. \quad (24)$$

Similar formulae can be written for $\hat{i}_{2A}$, $\hat{i}_{2B}$, and $\hat{i}_{2C}$, and their sum is

$$\hat{i}_{2S} = \hat{i}_{2A} + \hat{i}_{2B} + \hat{i}_{2C} = -3\frac{VI}{E}\cos\phi. \quad (25)$$

Equations (24) and (25) constitute proofs that the current in the dc link is time-invariant (property 1).

DC Power: The instantaneous power delivered by the dc voltage sources are

$$P = 0.5E(\hat{i}_{1S} - \hat{i}_{2S}) = 3VI\cos\phi. \quad (26)$$

AC Power: The instantaneous power received by the three ac voltage sources are

$$P = v_A i_A + v_B i_B + v_C i_C = 3VI\cos\phi. \quad (27)$$

From (26) and (27) one sees that the concept of "local average" current gives the correct formula for instantaneous power.

Step 3: Open Neutral Configuration

Applying the identity of (22), the neutral current

$$i_N = i_A + i_B + i_C = 0. \quad (28)$$

As such, the wire connecting the neutral of the wye to the center tap of the dc sources in Fig. 8 can be removed without affecting the results derived in step 2. On disconnecting this wire one has the bridge connection of Fig. 1.

Operation as a Static Capacitor: For $\phi = 270°$ the modulator operates as a static capacitor. Since $\cos 270° = 0$, from (24) and (25), the current in the dc link is zero. It is to be emphasized that the branch currents $\hat{i}_{1A}$, $\hat{i}_{1B}$, and $\hat{i}_{1C}$ are large, especially for large values of I. For instance

$$\hat{i}_{1A} = 0.707 I \sin(\omega t + 270°) - \frac{VI}{E} \cos(2\omega t + 270°). \quad (29)$$

However, the fundamental frequency and the second harmonic terms do not enter the dc link because of the trigonometric identities of (22) and (23). Physically it means that the reactive components of current circulate around the branches of the modulator. As such the dc link capacitor plays no part in contributing to the capacitive current. In general the fundamental frequency and the second harmonic terms in (21) account for the reactive components of current, and by virtue of (22) and (23), property 2 is observed.

Conclusion

The capability of the controlled-current PWM converter to deliver currents with near-sinusoidal waveforms at a leading power factor is a significant technical advance over the thyristor Graetz bridge. However, the subject is still in its infancy and much developmental work has to be done before the full potential can be realized.

Acknowledgment

J. C. Salmon thanks The Canadian Commonwealth Commission and J. W. Dixon thanks The Catholic University of Chile for the financial assistance that enabled them to undertake this research work. The authors are grateful to Professor H. C. Lee for the loan of certain equipment.

References

[1] T. Kataoka, K. Mizumachi, and S. Miyairi, "A pulsewidth controlled ac-to-dc converter to improve power factor and waveform of ac line current," *IEEE Trans. Ind. Appl.*, vol. IA-15, no. 6, pp. 670–675, Nov./Dec. 1979.

[2] D. Caroll, S. S. Abdel-Hamid, and F. Nozari, "A simplified analytical model for a current-fed force commutated converter," *IEEE Trans. Ind. Appl.*, vol. IA-16, no. 4, pp. 501–512, July/Aug. 1980.

[3] H. Zander, "Self-commutated rectifier to improve line conditions," in *Proc. IEEE*, vol. 120, no. 9, September 1973.

[4] N. Matsui and Y. Ohashi, "A microcomputer-based commutation failure free control system for the cascaded rectifier circuit," *IEEE Trans. Ind. Elect. Cont. Instr.*, vol. IECI-28, no. 4, pp. 380–387, Nov. 1981.

[5] Kocher and Steigerwald, "An ac-to-dc converter with high quality input waveforms," *IEEE Trans. Ind. Appl.*, vol. IA-19, no. 3, pp. 379–387, May/June 1983.

[6] P. D. Ziogas, Young-Goo Kang, and V. R. Stefanovic, "Optimum system design of a three-phase PWM rectifier-inverter type frequency changer," in *Conf. Rec. 1984 19th IAS Annual Meeting*, pp. 908–919.

[7] Y. Sumi, Y. Harumoto, T. Hasegawa, M. Yano, K. Ikeda, and T. Matsuura, "New static var control using force commutated inverters," *IEEE Trans. Power App. Syst.*, vol. PAS-100, no. 9, pp. 4216–4224, Sept. 1981.

[8] S. C. Peak and A. B. Plunkett, "Transistorized PWM induction motor drive system," *IEEE Trans. Ind. Appl.*, vol. IA-19, no. 3, pp. 379–387, May/June 1983.

[9] J. F. Eastham, A. R. Daniels, and R. T. Lipcznski, "A novel power inverter configuration," in *Conf. Rec. 1980, 15th IAS Annual Meeting*, pp. 748–751.

[10] John C. Salmon, "Three phase current controlled PWM inverter using bipolar transistors," M. Eng. thesis, May 1984, McGill University, Montreal, Canada.

Boon Teck Ooi (S'69–M'71–SM'85) received the B.Eng. Hons. degree from the University of Adelaide, Australia, the S.M. degree from the Massachusetts Institute of Technology, Cambridge, and the Ph.D. degree from McGill University, Montreal, PQ, Canada.

His research interests have included linear induction motors, electrodynamic magnetic levitation with superconducting magnets, subsynchronous resonance phenomena, stability of long distance power transmission, HVDC, and power electronics. He is presently a Professor in the Department of Electrical Engineering, McGill University, Canada.

John C. Salmon received the B.Sc.(Eng.) degree from Imperial College, London, UK, and the M.Eng. degree from McGill University, Montreal, PQ, Canada, in 1982 and 1984, respectively.

He has returned to Imperial College, where he is completing the requirements for the Ph.D. degree and where he is undertaking research into reliable inverter drives for induction motors and into the generation of modulation signals for voltage-fed ac drives.

Mr. Salmon was the holder of a Canadian Commonwealth Scholarship during his stay at McGill University.

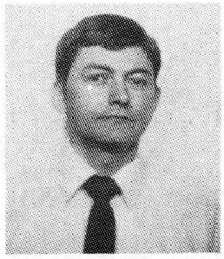

Juan W. Dixon was born in Santiago, Chile. He received the electrical engineering degree from the University of Chile in 1977. In 1986 he received the M.Sc. degree in electrical engineering from McGill University, Montreal, PQ, Canada.

From 1977 to 1979 he worked in Ferrocarriles del Estado, the Chilean national railways company, as a Chief of the Electrical Locomotives Section. Since May 1979 he has been working at the Catholic University of Chile as a Professor in electrical machines and power electronics. Presently, he is working towards the Ph.D. degree in electrical engineering at McGill University, Montreal, PQ, Canada.

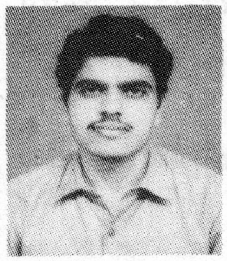

Ashok B. Kulkarni was born in Bangalore, India. He obtained the B.E. and M. Tech degrees from Bangalore University in 1981 and from the Indian Institute of Technology, Madras, in 1983, respectively, both in electrical engineering. He has recently completed the requirements for the M.Eng. degree in electrical engineering.

He worked with M/S Tata Consulting Engineers, Bangalore, during 1983–1984 as a Post Graduate Engineer. Since September 1984 he has been working as a Research Assistant at McGill University, Montreal, PQ, Canada.